A Study of Lifting Rotor Flapping Response Peak Distribution in Atmospheric Turbulence

G. H. Gaonkar*
Southern Illinois University, Edwardsville, Ill.

Studies are made of the peak statistics of rigid-blade flapping responses to atmospheric turbulence at high advance ratios. The rotor model is characterized by a finite dimensional linear system with periodically varying parameters and with feedback controls. System inputs represent a modulated nonstationary Gaussian process. The response description includes: 1) the ratio between the total number of peaks and of zero-level up-crossings per period, 2) the ranges of lower level thresholds within which the response process could deviate from being a narrow-band process, and 3) the accuracy of the approximate formulae of peak distribution conditional on the occurrence of a peak. The conditional probability density of peak magnitude indicates that high-level peaks which cause significant damage to system components are most likely to occur within narrow ranges of the azimuth angle. The Rayleigh density law provides a satisfactory approximation to this conditional probability density only within such narrow azimuth ranges. A similar approximation by a widely used narrow-band formula is not satisfactory. Numerical analysis further substantiates an earlier finding that the flapping response is a quasi-coherent narrow-band process with small phase angle variance.

Nomenclature

t	= nondimensional time
t_p	= particular value of t
ψ_k	= azimuth position of kth blade
N	= number of blades
B	= blade tip-loss factor
γ	= blade Lock number
μ	= rotor advance ratio
β_k	= flapping angle of kth blade
$\beta_0,\beta_1,\beta_{11}$	= multiblade flapping coordinates: coning, longitudinal and lateral cyclic flapping
θ_0	= collective pitch
λ	= inflow ratio or nondimensional vertical turbulence velocity
Ω	= angular rotor speed (rad/sec)
L	= turbulence scale length
R	= rotor radius
$P\Omega$	= natural flapping frequency
X	= vector with components $x_1,x_2,\ldots,x_p,\ldots$ etc.
$R_{XX}(t)$	= variance matrix of X with elements $R(x_ix_j)(t)$
$\sigma_{(xp)} = (R_{(xpxp)})^{1/2}$	= the standard deviation of x_p
U	= white noise vector
$M(t)$	= multiblade coordinate transformation matrix
$y_{(\beta 1)}(0,t)$	= unit gust response (β_1 in Eq. (19a) with $\lambda = 1$)
Ψ	= vector of multiblade coordinates
$R_{XF}(t)$	= $E[X(t)F^T(t)]$
K_0	= coning feedback gain
$\tan\delta_3$	= delta-three feedback gain
$E[N_{+(xp)}(\xi,t)]$	= expectation of the rate of up-crossings (from below) of the response component x_p with respect to threshold ξ.
$E[M_{(xp)}(\xi,t)]$	= the expected number of peaks of x_p per unit time above threshold level ξ.
$E[M_{(Txp)}(t)]$	= the expected rate of total number of peaks of x_p irrespective of magnitude.
$F_{(xp)}(\xi,t)$	= the probability distribution function of the peak magnitude of x_p conditional on the occurrence of a peak very close to t or "at t."
$p_{(xp)}(\xi,t) = d/d\xi F_{(xp)}(\xi,t)$	= the probability density function of the peak magnitude of x_p conditional on the occurrence of a peak very close to t.
I_n	= $n \times n$ identify matrix
$\{\ \}$	= column vector.
$[\ ]$	= row vector
$\simeq$	= approximately equal to

Received February 23, 1973; revision received November 26, 1973. Comments from K. H. Hohenemser, Washington University, St. Louis, and from Y. K. Lin, University of Illinois, Urbana, are gratefully acknowledged.

Index categories: VTOL Vibration; Structural Dynamic Analysis.

*Visiting Research Professor. Member AIAA.

1. Introduction

WITH the advent of high speed pure or convertible rotor craft and of large diameter propellers in V/STOL aircraft, the study of blade responses to atmospheric turbulence is an urgent requirement.[1-3] A recent development trend in helicopters is towards semihinged or 'hingeless' rotors having large radius blades of composite materials. Such configurations have the potential to provide improved maneuverability with greater control power and higher pay load because of reduced mechanical complexity and because of optimizing certain nonisotropic structural properties of fiber reinforced composites.[4-5] However, this increased control power is not without the increase of alternating root bending moments—leading to fatigue stresses. Significantly enough, blade stresses often reach their maximum near the hub, in the very region where pitch change and blade attachments occur. In general, such sophisticated configurations with increased blade number, hinge constraint, gust loading and advance ratio also exhibit increased gust sensitivity, ride roughness and fatigue stresses.[6-10] A comprehensive probabilistic description of these problems, at least in basic analytical aspects, requires the response descriptions in terms of root mean square values, the average rate of threshold crossings and peaks including probability density of peak magnitude.

Thus far, the response statistics of rotor blades to gust inputs include only root mean square values and threshold crossing expectations.[1,2,6,9,10] We also mention in passing that the quasi-coherent narrow-band features of the flapping response studied by Gaonkar and Hohenemser[1] are based on the threshold crossing expectations, assuming that the ratio of turbulence scale length over the rotor radius is extremely large. The present study is advanced over the preceding related works in several respects: 1) It considers the average number of flapping peaks per unit time, and the exact probability density function of flapping peak magnitude conditional on the occurrence of a peak. 2) It ascertains quantitatively the extent to which the rotor response is a periodic narrow-band process. In the sequel a parameter is evaluated, which is the ratio between the total number of peaks and zero-level up-cross-

ings per period. This parameter is used to describe the narrow-band features of the flapping response over one rotor revolution. For narrow-band processes an approximate peak distribution and certain reliability analysis are feasible with significantly reduced computational effort. 3) With the use of exact peak rates and peak density functions, it provides an appraisal of widely used narrow-band and Rayleigh density formulae. 4) It provides a computationally convenient formulation of generating response peak statistics. Such numerical aspects are of significance, since the rotor model represents a periodically varying system with multi-degrees of freedom of motion and with various control feedback systems.

For conventional low speed articulated rotors, dynamic loads from level flight cruising and maneuvering including unsteady aerodynamics are often adequate for gust loads. This study does not refer to conventional highly loaded helicopter rotors, but rather to low-lift high advance ratio compound rotor craft. In this regime, particularly for hingeless rotors, gust loadings are predominant.[1,2,9,10] Following Sissingh[7] we use for these flight conditions linear quasi-steady aerodynamics which includes reverse flow but excludes unsteady aerodynamics, nonuniform inflow and other nonlinear effects due to stall and compressibility. Extensive wind tunnel tests on frequency response by Kuczynski, Sharpe and Sissingh[8] have shown that such a linear aerodynamic theory is satisfactory for high advance ratio hingeless rotors. It is also during such high advance ratio flight regimes, that the rotor plane gust inputs with respect to rigid flapping responses are essentially represented by free atmospheric turbulence[9,10] which is approximately stationary and Gaussian.[11]

When the response process is nonstationary the statistical methods to assess the structural reliability are still in developmental stages. As shown in Ref. 12, the flapping response to atmospheric turbulence is a periodic nonstationary process. There still is much research needed to apply the studies of nonstationary response and other peak statistics to a routine design analysis. However, such studies would aid the development of approximate and yet reliable probabilistic techniques applicable to fatigue, ride roughness, and other dynamic analyses of rotor blades. Even though the numerical study is applied to rigid flapping oscillations, the response peak statistics are presented in a general format so as to be applicable to linear variable systems with Gaussian random inputs. With the feasibility of approximating a wide range of random loading histories as Gaussian, the developed methods are also of general interest to linearized dynamic problems of lifting rotor and V/STOL systems.

2. Variance Matrices of State Vector and Rate of Change of State Vector

Let $X(t)$ represent a $m \times 1$ state vector of a linear finite dimensional dynamic system with l degrees of freedom of motion. In general due to feedback etc. $m \geq 2l$. Partitioning the state vector into $X_1(t)$ and $X_2(t)$, consider the state equation of a $m \times m$ dynamic system under steady state conditions

$$\begin{Bmatrix} \dot{X}_1 \\ \dot{X}_2 \end{Bmatrix} = \begin{bmatrix} A_{11}(t) & A_{12}(t) \\ A_{21} & A_{22}(t) \end{bmatrix} \begin{Bmatrix} X_1 \\ X_2 \end{Bmatrix} + \begin{bmatrix} B_{11}(t) & B_{12}(t) \\ B_{21}(t) & B_{22}(t) \end{bmatrix} \begin{Bmatrix} F_1 \\ F_2 \end{Bmatrix} \quad (1a)$$

or in a compact form

$$\dot{X} = A(t)X + B(t)F \quad (1b)$$

where X_1 represents $2l$ response components or those state vector components which are subsequently subject to time variant linear transformations. $A(t)$ is a $m \times m$ state matrix representing the spring and damping parameters of the system including control feedback; while $B(t)$ is a $m \times n$ coupling matrix of input modulating functions. The $n \times 1$ random input vector $F(t)$ belongs to a stationary Gaussian process with zero mean values and with known covariance matrix $R_F(t_2 - t_1)$ or spectral density matrix $S_F(\omega)$. The stationary input process under steady state conditions is assumed to be generated by a physically realizable shaping filter system

$$\dot{F} = CF + DU \quad (2a)$$

which in terms of partitioning vectors F_1 and F_2 takes the form

$$\begin{Bmatrix} \dot{F}_1 \\ \dot{F}_2 \end{Bmatrix} = \begin{bmatrix} C_{11} & C_{12} \\ C_{21} & C_{22} \end{bmatrix} \begin{Bmatrix} F_1 \\ F_2 \end{Bmatrix} + \begin{bmatrix} D_{11} & D_{12} \\ D_{21} & D_{22} \end{bmatrix} \begin{Bmatrix} U_1 \\ U_2 \end{Bmatrix} \quad (2b)$$

where C and D are $n \times n$ constant matrices and where U is a $n \times 1$ white noise vector with the covariance matrix $I_n\delta(t_2 - t_1)$. Combining Eqs. (1b) and (2a) one gets

$$\dot{Z} = \begin{Bmatrix} \dot{X} \\ \dot{F} \end{Bmatrix} = \begin{bmatrix} A(t) & B(t) \\ 0 & C \end{bmatrix} \begin{Bmatrix} X \\ F \end{Bmatrix} + \begin{bmatrix} 0 \\ D \end{bmatrix} U \quad (3)$$

which is the steady-state equation of a $(m + n) \times (m + n)$ dynamic system with a state vector $Z(t)$. The state variance matrix of $Z(t)$ or $R_{ZZ} = E[Z(t)\, Z^T(t)]$, can now be obtained from the steady-state solution of the symmetric matrix equation[6,12]

$$\dot{R}_{ZZ} = R_{ZZ}\, \underset{\sim}{A}^T(t) + \underset{\sim}{A}(t)R_{ZZ} + \underset{\sim}{B}(t)\underset{\sim}{B}^T(t) \quad (4)$$

the number of unknowns being $(m + n)(m + n + 1)/2$.

For certain types of feedback mechanisms involving coupling effects between blades as well as in the treatment of rotor-fuselage system it is convenient to introduce a linear time variant transformation on certain components of the state vector. In lifting rotor studies such a transformation has been referred to as the generalized multiblade coordinates or complex coordinate representations.[13,14] For simplicity we will assume that the complete response vector $X_1(t)$ is expressed in terms of multiblade coordinates in real form.[13] The formal linear correspondence between the vector $X_1(t)$ and the $2l \times 1$ vector Ψ of blade coordinates is of the form

$$X_1(t) = M(t)\Psi(t) \quad (5)$$

where $M(t)$ is a $2l \times 2l$ matrix with periodic coefficients having closed form inverse matrix $M^{-1}(t)$ and derivative matrix $\dot{M}(t)$. By replacing X_1 and $\dot{X}_1$ in Eq. (1a) from Eq. (5), Eq. (3) in an explicit form reduces to

$$\dot{\bar{Z}} = \begin{Bmatrix} \Psi \\ \underline{X_2} \\ \underline{F_1} \\ F_2 \end{Bmatrix}^{\cdot} = \left[\begin{array}{c|c|c|c} -M^{-1}\dot{M} + M^{-1}A_{11}M & M^{-1}A_{12} & M^{-1}B_{11} & M^{-1}B_{12} \\ \hline -A_{21}M & A_{22} & B_{21} & B_{22} \\ \hline 0 & 0 & C_{11} & C_{12} \\ \hline 0 & 0 & C_{21} & C_{22} \end{array}\right] \begin{Bmatrix} \Psi \\ \underline{X_2} \\ \underline{F_1} \\ F_2 \end{Bmatrix} + \left[\begin{array}{c|c|c|c} 0 & 0 & 0 & 0 \\ \hline 0 & 0 & 0 & 0 \\ \hline 0 & 0 & D_{11} & D_{12} \\ \hline 0 & 0 & D_{21} & D_{22} \end{array}\right] \begin{Bmatrix} 0 \\ \underline{0} \\ \underline{U_1} \\ U_2 \end{Bmatrix} \quad (6)$$

where $\bar{Z}$ represents the transformed state vector. The transformed state variance matrix equation or $R_{\bar{Z}\bar{Z}}$ obtainable from Eq. (6) is analogous to Eq. (4) with X_1 replaced by Ψ and Z by $\bar{Z}$. From Eq. (5), the response variance matrix $R_{(X1X1)}$ and the cross-variance matrix $R_{(X1F)}$ are computed from the relations

$$R_{(X1X1)}(t) = M(t)\, R_{\Psi\Psi}(t)M^T(t) \quad (7a)$$

$$R_{(X1F)}(t) = M(t)\, R_{\Psi F}(t) \tag{7b}$$

For computing the expected values of threshold crossing rates it is sufficient to obtain the variance matrix between x_p and $\dot{x}_p$, where x_p is a typical response component. Such 2 × 2 variance matrices of different response components are submatrices of the response variance $R_{(X1X1)}$. However, the expected values of the peak (or trough) rates of x_p requires the 3 × 3 symmetric matrix between x_p, $\dot{x}_p$ and $\ddot{x}_p$, among which only the three elements $R_{(xpxp)}$, $R_{(xp\dot{x}p)}$ and $R_{(\dot{x}p\dot{x}p)}$ are directly obtainable from the response variance matrix $R_{(X1X1)}$. From a typical row of the state equation with $\dot{x}_i = \dot{x}_p$

$$\ddot{x}_p = \dot{x}_i = \lfloor a_{ij} \rfloor \{x_j\} + \lfloor b_{ik} \rfloor \{f_k\}, \quad j = 1, 2, \ldots m \quad k = 1, 2, \ldots, n, \; m \geq n \tag{8a}$$

where indexes i and p are prefixed.

Premultiplying both sides of Eq. (8a) with x_p, $\dot{x}_p$ and $\ddot{x}_p$ respectively and then taking the expectations, one obtains

$$R_{(xp\ddot{x}p)} = R_{(xp\dot{x}i)} = \lfloor a_{ij} \rfloor \{R_{(xpxj)}\} + \lfloor b_{ik} \rfloor \{R_{(xpfk)}\} \tag{8b}$$

$$R_{(\dot{x}p\ddot{x}p)} = R_{(xi\dot{x}i)} = \lfloor a_{ij} \rfloor \{R_{(xixj)}\} + \lfloor b_{ik} \rfloor \{R_{(xifk)}\} \tag{8c}$$

and

$$R_{(\ddot{x}p\ddot{x}p)} = R_{(\dot{x}i\dot{x}i)} = \lfloor a_{ij} \rfloor [R_{(xjxq)}] \{a_{iq}\} + \lfloor a_{ij} \rfloor [R_{(xjfr)}] \{b_{ir}\} + \lfloor b_{ik} \rfloor [R_{(fkxq)}] \{a_{iq}\} + \lfloor b_{ik} \rfloor [R_{(fkfr)}] \{b_{ir}\} \quad j, q = 1, 2, \ldots, m \quad k, r = 1, 2, \ldots, n. \tag{8d}$$

Observe that all the variance matrix elements on the right hand side of Eqs. (8b–d) are actually contained in the state variance matrix R_{ZZ}.

3. Response Threshold Crossing and Peak Statistics

For direct reference purposes in the subsequent description of numerical results, we briefly mention three basic formulations of threshold upcrossing and peak distribution statistics. The first two formulations, due to Rice, refer to the expected number of threshold up-crossings and of peaks per unit time. The third formulation, due to Howell and Lin, concerns the probability density of peak magnitude conditional on the occurrence of a peak.[15-18] The random function under consideration is a typical component of the response vector of a linear system subject to Gaussian inputs with zero mean values. Therefore the response vector is also Gaussian with zero mean values and the response correlation matrix is identical to the response covariance matrix. In the interest of notational simplicity, the subtle difference between the sample functions and the associated random process is also suppressed. The expected rate of up-crossings of threshold level ξ by a response component x_p is given by[1,17]

$$E[N_{(+xp)}(\xi, t)] = \sigma_{(xi)} \left[(2\pi\, \sigma_{(xp)}) \right]^{-1} (1 - r_{(xpxi)}^2)^{1/2} \times \exp(-\eta^2/2)[\exp(-\nu^2) + \pi^{1/2}\nu(1 + \operatorname{erf}\nu)] \tag{9a}$$

where x_i is equal to $\dot{x}_p$ and $\eta = \xi/\sigma_{(xp)}$. The error function erf (θ), the correlation coefficient $r_{(xpxi)}$ and ν are

$$\operatorname{erf}(\theta) = \frac{2}{(\pi)^{1/2}} \int_0^{\theta} e^{-t^2}\, dt,$$

$$r_{(xpxi)} = \frac{E[x_p x_i]}{\sigma_{(xp)}\sigma_{(xi)}}$$

With $\xi = 0$ in Eq. (9), the expected number of up-crossings per unit time at the zero level simplifies to

$$E[N_{(+xp)}(O, t)] = (1 - r_{(xpxi)}^2)^{1/2}\sigma_{(xi)}/(2\pi\sigma_{(xp)}) \tag{9b}$$

By differentiating both sides of Eq. (9a) with respect to ξ, the rate of change of average threshold up-crossing rate with respect to amplitude level takes the form

$$\frac{\partial}{\partial \xi} E[N_{(+xp)}(\xi; t)] = -E[N_{(+xp)}(O, t)]\{(\sigma_{(xp)})^{-1} \exp(-\eta^2/2) \times [\eta \exp(-\nu^2) - (\pi)^{1/2}\nu(\eta^{-1} - \eta)(1 + \operatorname{erf}\nu)]\} \tag{10}$$

The expected number of peaks per unit time above threshold level ξ is given by[15]

$$E[M_{(xp)}(\xi, t)] = -\int_{\xi}^{\infty} dx_p \int_{-\infty}^{0} \ddot{x}_p\, p_{(xp\dot{x}p\ddot{x}p)}(x_p, o, \ddot{x}_p, t) d\ddot{x}_p \tag{11}$$

With χ representing the vector with components $x_p, \dot{x}_p$ and $\ddot{x}_p$, the joint probability density function $p_{(xp\dot{x}p\ddot{x}p)}$ has the form

$$p_\chi(\chi; t) = p_{(xp\dot{x}p\ddot{x}p)}(x_p, \dot{x}_p\ddot{x}_p; t) = (2\pi)^{-3/2} |\Lambda_\chi|^{-1/2} \exp\{-\frac{1}{2}\chi^T \Lambda_\chi^{-1}\chi\} \tag{12}$$

where $|\Lambda_\chi|$ is the determinant of the variance matrix of χ, and $|\Lambda_\chi|^{-1}$ is the corresponding inverse matrix having α_{jk} as the (j,k) element. In the study of expectation of peak rates and of conditional peak magnitude distributions, it is sufficient to compute α_{11}, α_{13} and α_{33}

$$\alpha_{11} = [(R_{(\dot{x}p\dot{x}p)}R_{(\ddot{x}p\ddot{x}p)} - R^2_{(\dot{x}p\ddot{x}p)})]/|\Lambda_\chi| \tag{13a}$$

$$\alpha_{13} = [(R_{(xp\dot{x}p)}R_{(\dot{x}p\ddot{x}p)} - R_{(xp\ddot{x}p)}R_{(\dot{x}p\dot{x}p)})]/|\Lambda_\chi| \tag{13b}$$

$$\alpha_{33} = (R_{(xpxp)}R_{\dot{x}p\dot{x}p} - R^2_{(xp\dot{x}p)})|\Lambda_\chi| \tag{13c}$$

By substituting Eq. (13) into Eq. (12) and setting $\xi = -\infty$ in Eq. (11), the expected rate of total number of peaks irrespective of magnitudes simplifies to

$$E[M_{(Txp)}(t)] = E[M_{(xp)}(-\infty, t)] = (2\pi)^{-1}(\alpha_{11}/|\Lambda_\chi|)^{1/2}/(\alpha_{11}\alpha_{33} - \alpha_{13}^2) \tag{14}$$

In a sufficiently small time interval $(t,\ t + \Delta t)$, the ratio, Prob. {two or more peaks occur in $(t, t + \Delta t)$}/ Prob. {one peak occurs in $(t, t + \Delta t)$}, has a sufficiently small value. Further, $E[M(x_p)(\xi,t)]\ \Delta t$ and $E[M_{(Txp)}(t)]\Delta t$ respectively represent in the interval $(t, t + \Delta t)$, the probability of occurrence of one peak above threshold level ξ and the probability of occurrence of one peak irrespective of magnitude. Therefore, the expression $\{1 - (E[M(\xi,t)]\Delta t/E[M_T(t)\Delta t)\}$ gives the probability that in $(t, t + \Delta t)$ the peak is less than or equal to ξ given that such a local peak occurs at t[17]. Then, the probability distribution function of peak magnitude conditional on the occurrence of a peak can be expressed as[17]

$$F_{(xp)}(\xi, t) = 1 - \frac{E[M_{(xp)}(\xi, t)]}{E[M_{(Txp)}(t)]} \tag{15}$$

By differentiating Eq. (15) with respect to ξ, and considering Eqs. (11) and (14) the conditional probability density of peak magnitude reduces to[17]

$$p_{(xp)}(\xi, t) = (2\pi)^{-1/2}[\alpha_{11}^{1/2} - \alpha_{13}^2/(\alpha_{11}^{1/2}\alpha_{33})] \times \{\exp(-\alpha_{11}\xi^2/2) + \xi(\pi/2)^{1/2}(\alpha_{13}/\alpha_{33}^{1/2}) \times \exp[-(\alpha_{11} - \alpha_{13}^2/\alpha_{33})\xi^2/2] \times [1 + \operatorname{erf}(2^{-1/2}\alpha_{33}^{-1/2}\alpha_{13}\xi)]\} \tag{16}$$

where α_{11}, α_{13} and α_{33} are given by Eq. (13). Observe that $p_{(xp)}(\xi,t)$ is set to zero when the probability that one peak occurs in $(t, t + \Delta t)$ is exactly equal to zero. For physical processes, it is plausible that the value of $p_{(xp)}(\xi,t)$ is almost negligible when the occurrence of a peak in $(t, t +$

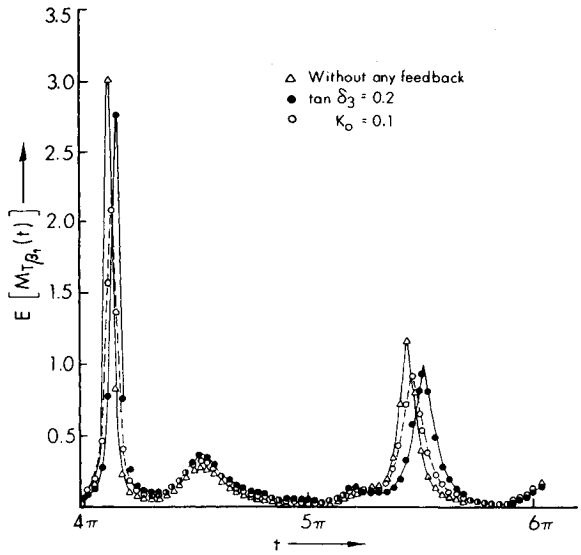

Fig. 1 Average number of total flapping peaks per unit time.

Δt) is very close to being an unlikely event.

In certain peak distribution studies of narrow-band processes, it is assumed that $E[M_{(xp)}(\xi,t)] \simeq E[N_{+(xp)}(\xi,t)]$, and the probability density of peak magnitude conditional on the occurrence of a peak is further approximated by[15]

$$p_{(xp)}(\xi,t) \simeq -\frac{\partial}{\partial \xi} E[N_{(+xp)}(\xi,t)]/E[N_{(+xp)}(o,t)] \quad (17)$$

When $E[N_{+(xp)}(\xi,t)]$ decreases with increasing threshold levels, which apparently is the case for ideal and non-stationary narrow-band processes, $p_{(xp)}(\xi,t)$ from Eq. (17) is nonnegative. Here the term ideal implies that

$$\frac{\partial}{\partial \xi} E[M_{(xp)}(\xi,t)] = \frac{\partial}{\partial \xi} E[N_{(+xp)}(\xi,t)]$$

Another expression which is a special case of the Weibull density expression is the Rayleigh density law:

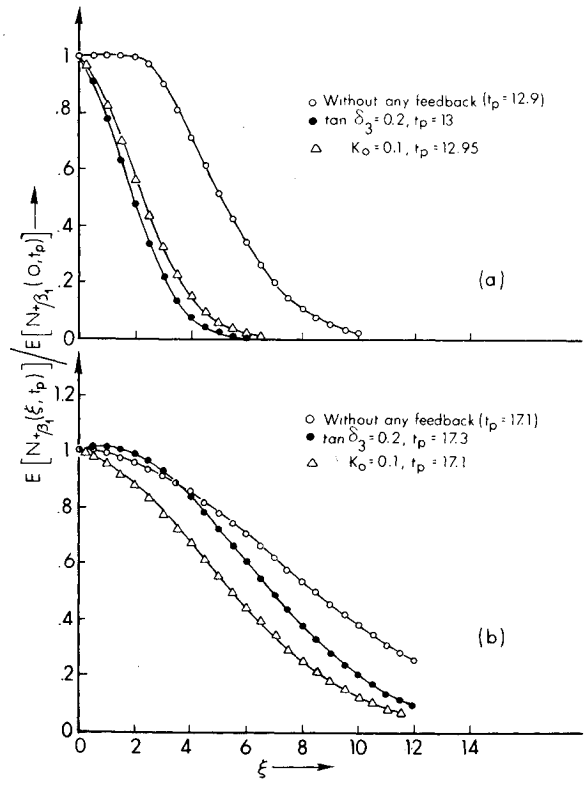

Fig. 2. Average threshold up-crossing rate variations at the most likely instances of peak occurrence

$$p_{(xp)}(\xi,t) = \xi(\sigma_{(xp)}(t))^{-2} \exp(-\xi^2/2\sigma_{(xp)}{}^2(t)), \quad 0 \le \xi < \infty \quad (18)$$

4. Description of the Rotor Model

For illustrative purposes, consider a lifting rotor model having three untwisted rigid flapping blades with elastically restrained flapping hinges at the rotor center. Following Refs. 7 and 13 the linearized equations of the kth blade with delta three and coning feedback read

$$\dot{X}_1 =$$

$$\begin{Bmatrix} \beta_k \\ \dot{\beta}_k \end{Bmatrix}^{\cdot} = \begin{Bmatrix} x_1 \\ x_j \end{Bmatrix}^{\cdot} = \begin{bmatrix} 0 & 1 \\ -\Omega^2(P + \frac{\gamma}{2} k(\psi_k) & -\frac{\gamma}{2}\Omega c(\psi_k) \\ 0 & 0 \end{bmatrix} \begin{Bmatrix} x_i \\ x_j \end{Bmatrix}$$

$$+ \begin{bmatrix} \frac{\gamma}{2}\Omega^2 m_{(\theta 0)}(\psi_k) & \frac{\gamma}{2}\Omega^2 m_\lambda(\psi_k) \end{bmatrix} \begin{Bmatrix} \theta_0 \\ \lambda \end{Bmatrix} \quad (19a)$$

$$\theta_0 = -\tan \delta_3 \beta_k \quad (19b)$$

and

$$\theta_0 = -K_0\beta_0 = -K_0 \frac{1}{3} \sum_k \beta_k;\ k = 1, 2 \text{ and } 3 \quad (19c)$$

where P represents the blade flapping restraint parameter which is equal to one in the free flapping case; and $P\Omega$, the natural flapping frequency. For blades with root restraint the value of P is larger than one, increasing with decreasing rotor angular speed. Hence forth, Ω will be normalized to unity so that the period of one rotor revolution is 2π and the azimuth position of the kth blade in terms of a nondimensional time unit t is given by

$$\psi_k = \frac{2\pi}{3}(k-1) + t, \qquad k = 1, 2, \text{ and } 3 \quad (20)$$

The time variable system and input parameters in Eq.

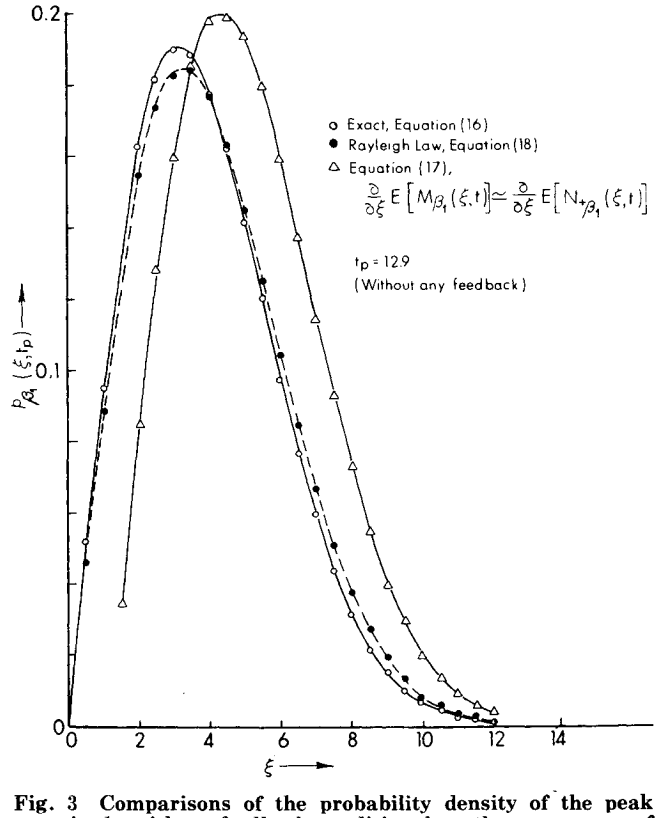

Fig. 3 Comparisons of the probability density of the peak magnitude without feedback conditional on the occurrence of a peak at t = 12.9.

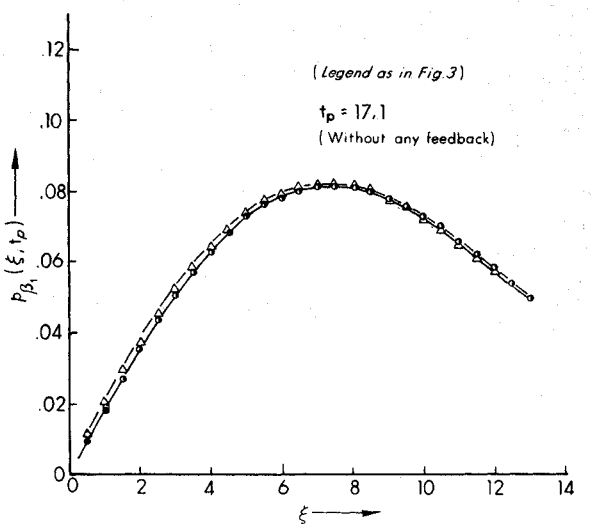

Fig. 4 Comparisons of the probability density of the peak magnitude without feedback conditional on the occurrence of a peak at t = 17.1.

(19a) are dimensionless, periodic functions, continuous but nonanalytic. In particular, $k(\psi_k)$ and $c(\psi_k)$ are aerodynamic blade stiffness and damping functions; $m_{(\theta 0)}(\psi_k)$ and $m_\lambda(\psi_k)$ are modulating functions to collective pitch and inflow excitations. For further details on the listings of these functions applicable to different flow regions, see Ref. 7.

While considering the rotor system with coning feedback, Eqs. (19a) and (19c), we express the flapping response components β_1, β_2 and β_3 in terms of corresponding multiblade flapping coordinates—namely, the coning angle β_0, the longitudinal and lateral cyclic angles β_I and β_{II}. Referring to Eq. (5), the particular transformations matrix is:[13]

$$M(t) = \begin{bmatrix} 1 & \cos\psi_1 & \sin\psi_1 \\ 1 & \cos\psi_2 & \sin\psi_2 \\ 1 & \cos\psi_3 & \sin\psi_3 \end{bmatrix} \tag{21}$$

whose closed form inverse matrix simplifies to

$$M^{-1}(t) = \frac{1}{3}\begin{bmatrix} 1 & 1 & 1 \\ 2\cos\psi_1 & 2\cos\psi_2 & 2\cos\psi_3 \\ 2\sin\psi_1 & 2\sin\psi_2 & 2\sin\psi_3 \end{bmatrix} \tag{22}$$

where ψ_k is given by Eq. (20).

It is observed in passing that Eqs. (19a) and (19b) are also applicable to multibladed models. Due to the absence of coupling effects between blades such systems could be treated with the single blade analysis. However, in the interest of uniform comparison with the study of Eqs. (19a) and (19c) using the transformation in Eq. (21), the discussion of all numerical results will be restricted to three-bladed configurations.

5. Numerical Scheme

This study refers to rigid flapping responses at a high rotor advance ratio due to free atmospheric vertical turbulence velocities at the rotor centre. Three bladed rotors with zero feedback and with delta-three feedback comprise the first two numerical examples and are treated with the single blade analysis. The state representation is given by Eq. (19a) with k = 1; θ_0 is set to zero with zero feedback and θ_0 is replaced by Eq. (19b) to include delta-three feedback. The stochastic model of vertical turbulence velocities λ in Eq. (19a), is identical to the one developed in Ref. 1, in which, as an approximation to the Taylor-von Kármán expression, an exponential spectrum is assumed. Under steady-state conditions the scalar shaping filter system is given by Eq. (2a) with F replaced by the scalar λ, and where $C = 2\mu/(L/R)$ and $D = 2(\mu/(L/R))^{1/2}$. In the third numerical example, a three bladed rotor with coning feedback is treated; the original state equation is obtained from Eq. (19a) with k = 1, 2, and 3 and with $m = 2l = 6$. The transformed state equation in terms of blade coordinates is obtained when the response components β_1, β_2, and β_3 are expressed in terms of β_0, β_I and β_{II} using the transformation according to Eq. (21), and by replacing θ_0 by $K_0\beta_0$.

The system parameter functions $c(\psi_k)$, $k(\psi_k)$ etc. in Eq. (19a) were approximated by finite Fourier series with a truncation error less than 0.01%. As observed earlier, these system parameter functions, though nonanalytic, are continuous functions of the azimuth angle. Therefore, the Fourier series approximations should be viewed in the context of simplifying the algebra and other programming details of response peak rate expectations. A Runge-Kutta method is used to integrate the state variance matrix Eq. (4). However, when blade coordinates are used, the solution refers to the transformed state variance matrix equation obtained from Eq. (6), followed by additional matrix manipulations according to Eq. (7). The response process, though nonstationary; is periodic under steady state conditions.[6,12] Therefore the threshold crossing and peak statistics of β_1 are presented only during the steady state third revolution. $R_{(\beta 1 \beta 1)}$, $R_{(\beta 1 \dot\beta 1)}$, and $R_{(\dot\beta 1 \dot\beta 1)}$ are directly available from the state variance matrix; the other three elements $R_{(\beta 1 \ddot\beta 1)}$, $R_{(\dot\beta 1 \ddot\beta 1)}$ and $R_{(\ddot\beta 1 \ddot\beta 1)}$ are computed according to Eqs. (8b-d). Having thus obtained the six elements of the symmetric variance—covariance matrix between β_1,$\dot\beta_1$ and $\ddot\beta_1$, the three elements of the corresponding inverse matrix, α_{11}, α_{13} and α_{33}, are obtained from Eq. (13), which are required to evaluate Eqs. (14) and (16). A numerical quadrature based on Simpson's formula is used to compute the total number of threshold upcrossings and peaks per rotor revolution.

6. Discussion of Computer Results

In combination with the input parameters L/R = 12 and σ_λ = 1 the graphically presented numerical results are for the system constants: μ = 1.6, γ = 8, B = 0.97, P = 1.15, $\tan\delta_3$ = 0.2 and K_0 = 0.1. The flapping system is well within the stability region without or with the inclusion of delta-three or coning feedback system.[13]

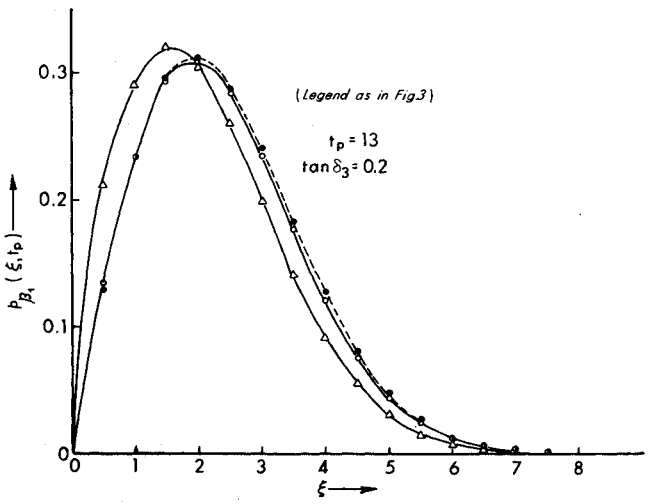

Fig. 5 Comparisons of the probability density of the peak magnitude with delta-three feedback conditional on the occurrence of a peak at t = 13.

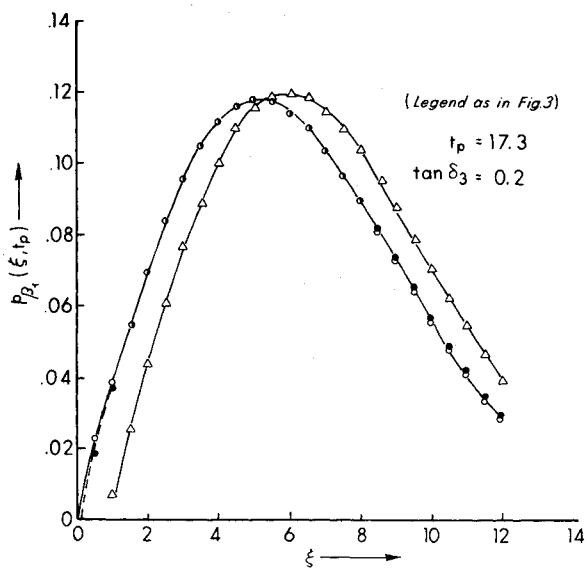

Fig. 6 Comparisons of the probability density of the peak magnitude with delta-three feedback conditional on the occurrence of a peak at $t = 17.3$.

Figure 1 shows the expectation of the total number of peaks per unit time according to Eq. (14). In the single-blade analysis with zero feedback, two sharp peaks or spike shaped local maxima of $E[M_{(T\beta_1)}(t)]$ occur at 12.9 and 17.1. Similar spike shaped local maxima occur at 18.0 and 17.3 with delta-three feedback, and at 12.95 and 17.2 with coning feedback. For these three cases in general, one of the locations of sharp peaks is about a quarter quadrant after the aft position which is at $t = 0, 2\pi, 4\pi, \ldots$, etc; the second location is close to the center-position of the reversed flow region when the azimuth position corresponds to $3\pi, 5\pi, \ldots$, etc. The area under the curve in figure 1 is concentrated within two narrow ranges of the azimuth angle, each range being centered at about the location of the local maximum of $E[M_{(T\beta_1)}(t)]$.

From Fig. 1, it is evident that most of peaks are likely to occur within narrow ranges of the azimuth angle. We also mention that the absolute value of the response to unit gust, or $|y_{(\beta_1)}(0,t)|$, and the standard deviation of the response, or $\sigma_{(\beta_1)}(t)$, have two local maxima per period and that the locations of these maxima are very close to those of $E[M_{(T\beta_1)}(t)]$.[6,13] Further, the variation of $E[M_{(T\beta_1)}(t)]$ is similar to that of $E[N_{+(\beta_1)}(0,t)]$[1,6] which also exhibits two sharp peaks per period. These observations concerning the spike shaped distributions of $E[M_{(T\beta_1)}(t)]$ within particular azimuth-ranges further subtantiate an earlier finding that the flapping response to gust inputs is a quasi narrow-band process with small phase angle variance. In other words, for finite values of L/R, peaks can occur at any azimuth location, with the most likely occurrences close to those for $L/R = \infty$[1].

Independent of the inclusion of feedback controls, the total number of peaks per period is close to 1.3, which is the area under the corresponding curve in Fig. 1 between 4π and 6π. It is known that the total number of flapping up-crossings of zero-level is equal to one per period.[1,6] Because in one rotor revolution, the ratio of total number of peaks to total number of zero-level up-crossings is much less than 2, the flapping response process could be approximately treated as a narrow-band process. In conjunction with this approximation the fact that the values of $E[M_{(T\beta_1)}(t)]$ are concentrated within two narrow azimuth-ranges per period can also be expressed by stating that the peak values for large numbers of response sample functions occur within one of these ranges. However, the observation that the total number of peaks is about 30% higher than the total number of zero-level up-crossings per period merits further discussion. This observation indicates that the flapping response process slightly deviates from a narrow-band process and that the occurrence of more than one peak per period for a small number of sample functions is plausible.

For a nonstationary process, a ratio of $E[M_{(T\beta_1)}(t)]/E[N_{+(\beta_1)}(0,t)]$ which is considered small enough to justify a narrow-band assumption has not been established; nor are the limiting values of this ratio known when either a Rayleigh or a Gaussian approximation is justifiable.[19] Therefore we consider three related aspects of the response process 1) the ranges within which the response deviates from a narrow-band process, 2) the extent to which the Rayleigh density law and the narrow-band approximation according to Eq. (18) provide a satisfactory approximation of $p_{(\beta_1)}(\xi,t)$, and 3) the description of $p_{(\beta_1)}(\xi,t)$ during one rotor revolution to further investigate the quasi narrow-band features of the response. For a quantitative description we stipulate that thresholds less than or equal to 0.2 $[(\sigma_{(\beta_1)})]_{\max}$ are lower level and in the neighborhood of $[(\sigma_{(\beta_1)})]_{\max}$ or greater are higher level, where $[(\sigma_{(\beta_1)})]_{\max}$ refers to the absolute maximum of $\sigma_{(\beta_1)}(t)$ in one rotor revolution. It is mentioned in passing that $[(\sigma_{(\beta_1)})]_{\max}$ is equal to 7.4 in the first example with neither delta-three nor coning feedback and for the remaining two cases $(\sigma_{(\beta_1)})_{\max}$ is close to 5.4. In Figs. 2–8, t_p represents two particular azimuth locations at which the sharp peaks of $E[M_{(T\beta_1)}(t)]$ occur. As observed earlier most of the peaks are likely to occur within the neighborhood of these two azimuth positions. Figure 2a shows that in the first example $E[N_{+(\beta_1)}(\xi,t)(\xi,12.90)]$ does not decrease with the increase in ξ up to $\xi \leq 1.5$. Also, a similar variation up to $\xi \leq 1$ is observed in $E[N_{+(\beta_1)}(\xi,t)(\xi,17.30)]$, see Fig. 2b. From Figs. 2a and 2b, it is evident that up to certain lower level thresholds, depending upon particular configurations, $E[N_{+(\beta_1)}(\xi,t)(\xi,t_p)]$ does not always decrease with the increase in ξ. Consequently, up to such lower level thresholds, the rate of change of $E[N_{+(\beta_1)}(\xi,t)(\xi,t_p)]$ with respect to ξ is not always negative. This means Eq. (17) is not applicable up to certain lower level thresholds, for this would violate the non-negativity requirement. For the configurations studied, such lower level thresholds are smaller than $0.2(\partial_{(\beta_1)}(t))_{\max}$ in magnitude.

In Figs. 3–8, the values of $P_{(\beta_1)}(\xi,t_p)$ from Eq. (16) are shown, and they are compared with the corresponding Rayleigh and narrow-band approximations, Eqs. (18) and (17). In particular, Figs. 3 and 4 show the variations of $p_{(\beta_1)}(\xi,12.9)$ and $p_{(\beta_1)}(\xi,17.1)$ for the first example with zero feedback. Although it appears from Fig. 4 that approximation from Eq. (17) is satisfactory, Fig. 3 clearly shows that this approximation could introduce substantial errors—even within the ranges of higher thresholds. How-

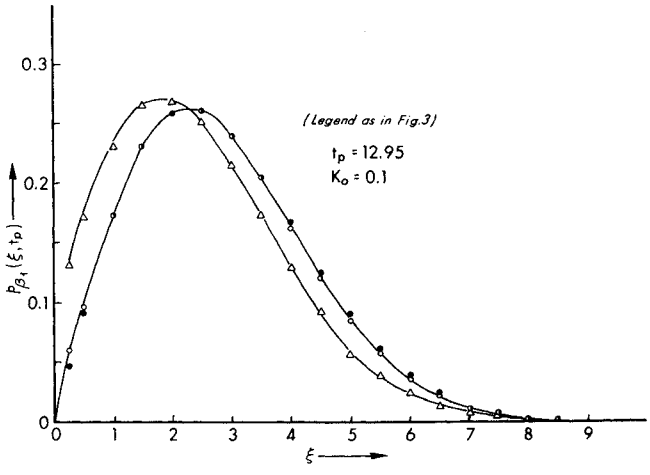

Fig. 7 Comparisons of the probability density of the peak magnitude with coning feedback conditional on the occurrence of a peak at $t = 12.95$.

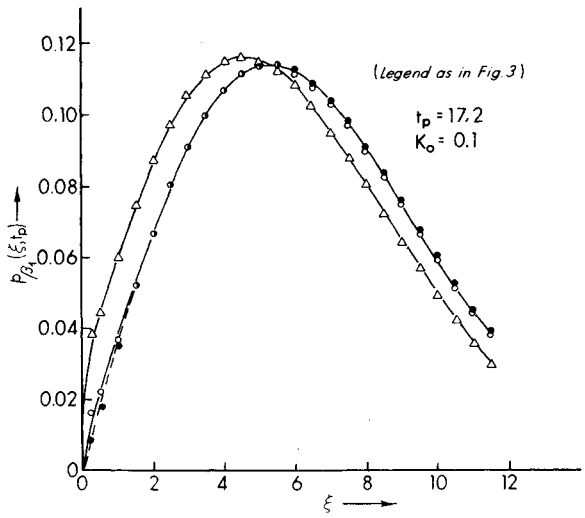

Fig. 8 Comparisons of the probability density of the peak magnitude with coning feedback conditional on the occurrence of a peak at t = 17.2.

ever, the Rayleigh density expression is in excellent agreement with the exact formula from Eq. (16). Similar conditional probability density functions of peak magnitude shown in Figs. 5 and 6 refer to the second example with delta-three feedback. Here also the approximation given by Eq. (17) is not satisfactory, whereas results from Eq. (18) are almost indistinguishable from the exact results. The nonapplicability of Eq. (17) up to $\xi \leq 1$ in $p_{(\beta 1)}(\xi,17.3)$ is consistent with Fig. 2b in which $(d/d\xi)E[N_{(+\beta 1)}(\xi,17.3)]$ is not negative up to $\xi \leq 1$. Figures 7 and 8 referring to the third example with coning feedback also show that Eq. (17) is not satisfactory and that the Rayleigh density law is almost equivalent to the exact formulation for the selected t_p values.

Because approximations of the type given by Eq. (17) are used in the peak statistics of "narrow-band type" processes and because one such approximation seems to introduce substantial errors in the present study, certain general comments in this context appear in order. Above the ranges of certain lower level thresholds, the integrated

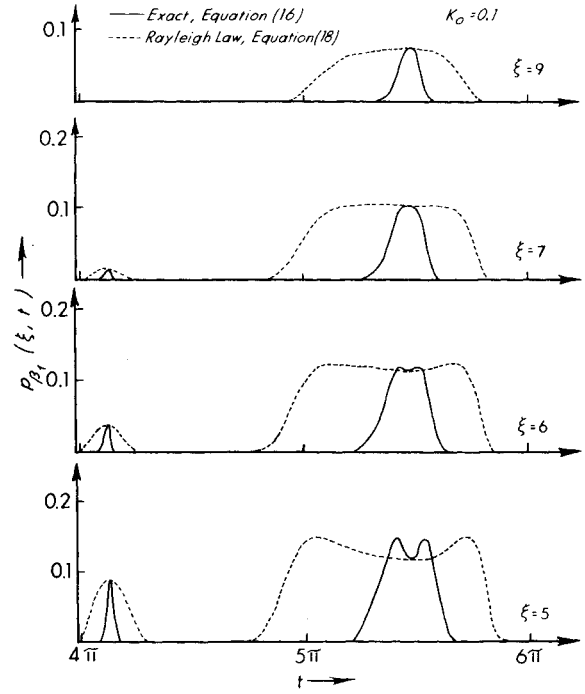

Fig. 9 The conditional probability density of the peak magnitude and the Rayleigh density law for different azimuth locations.

Table I Parameter combination.

	μ = 1.6, B = 0.97, N = 3, L/R = 12 and 32, σ_λ = 1					
γ	4	4	8	8	8	8
p	1.15	1.15	1.3	1.3	1.15	1.15
$\tan\delta_3$	0.2	0	0.2		0	0
K_0	0	0.1	0	0.1	0	0.15

value of $E[N_{(+\beta 1)}(\xi,t)]$ over one rotor revolution seems to provide a good approximation to the corresponding total number of peaks. It is in general difficult to assess the quantitative error in approximating $E[M_{(\beta 1)}(\xi,t)]$ by $E[N_{+(\beta 1)}(\xi,t)]$. The present study however shows that the approximation of $\partial/\partial\xi\ E[M_{(\beta 1)}(\xi,t)]$ by $(\partial/\partial\xi)$ $E[M_{+(\beta 1)}(\xi,t)]$ at $t = t_p$ is not satisfactory for rotor response processes. After all, the comparison of Eq. (17) with Eq. (16) is essentially a comparison between $(\partial/\partial\xi)$ $E[M_{(\beta 1)}(\xi,t)]$ and $(\partial/\partial\xi)$ $E[N_{+(\beta 1)}(\xi,t)]$, because $E[M_{(T\beta 1)}(t)]$ and $E[N_{+(\beta 1)}(0,t)]$ at $t = t_p$ could be treated as corresponding scaling constants, though differing in magnitude.

For the third example with coning feedback, Fig. 9 shows $p_{(\beta 1)}(\xi,t)$ between 4π and 6π for high level thresholds 5–7, and 9. The values of $p_{(\beta 1)}(\xi,t)$ from Eq. (16) exhibit two bell shaped distributions centered at about the locations of the local maxima of $\sigma_{(\beta 1)}(t)$ or $E[M_{(T\beta 1)}(t)]$. With increasing thresholds one of the bell shaped distributions disappears and only the primary distribution centered at the location of $[(\sigma_{(\beta 1)}(t))]_{\max}$ remains. The variation of $p_{(\beta 1)}(\xi,t)$ during one rotor revolution is somewhat similar to that of $E[N_{+(\beta 1)}(\xi,t)]$. However, unlike $E[N_{+(\beta 1)}(\xi,t)]$, the values of $p_{(\beta 1)}(\xi,t)$ are symmetrically distributed and are concentrated within much narrower azimuth ranges. Also the area under the curve in Fig. 9 between 4π and 6π is about 35 to 40% less than the corresponding area with respect to $E[N_{+(\beta 1)}(\xi,t)]$. For high level thresholds, the fact that values of $p_{(\beta 1)}(\xi,t)$ are concentrated within two extremely narrow azimuth ranges is consistent with the quasi-narrow-band features of the response process.[1] From Fig. 9, it is evident that the Rayleigh density law is a good approximation to $p_{(\beta 1)}(\xi,t)$ from Eq. (16) only within narrow azimuth ranges and not for all azimuth locations. However, as observed earlier, most of the peaks are likely to occur within such narrow azimuth ranges.

The over-all findings of this study were further substantiated by an additional set of computations. The particular parameter values assumed for the stable three-bladed configuration are shown in Table 1.

7. Conclusions

The study of blade response statistics due to atmospheric turbulence has been extended here to include the expectation of total number of peak rates, the probability density functions conditional on the occurrence of a peak, and to provide a general method of appraising approximate peak distribution formulations. Computationally, the exact treatment of this conditional probability density of peak magnitude is essentially no more involved than the corresponding methods using $(\partial/\partial\xi)\ E[M_{(\beta 1)}(\xi,t)] \simeq (\partial/\partial\xi)\ E[N_{+(\beta 1)}(\xi,t)]$. It is shown that such an approximation which also leads to probability density functions conditional on the occurrence of a peak, is not satisfactory for rotor response processes.

The following detailed conclusions are based on the study of a linearized dynamic problem of a lifting rotor with three rigid flapping blades having elastically restrained flapping hinges at the rotor centre, and with coning or delta-three control feedbacks, assuming high advance ratio and low-rotor lift flight regimes with uniform inflow on the rotor disk:

1) Within the ranges of lower-level thresholds, the periodic response process could deviate from being a strictly narrow-band process in the sense that the rate of change of an average threshold crossing rate with respect to threshold is not negative. The magnitude of such lower level thresholds is less than $0.2[\sigma_{(\beta 1)}]_{max}$. This finding is of significance in the studies of cumulative damage and vibration control which are practically independent of low amplitude responses.

2) In one rotor revolution, the total number of flapping peaks is much less than 2; it is about 25 to 35% higher than the total number of zero-level up-crossings which is equal to one. The flapping response process, excluding in certain cases small ranges of lower level thresholds, could adequately be represented by a periodic narrow-band process. Hence, further development of the stochastic treatment of blade reliability analyses concerning fatigue and ride roughness becomes relatively simplified.[20]

3) The changes in the values of Lock number, flapping frequency parameter and gain factors do not appreciably alter the over-all stochastic features of the flapping response process, particularly concerning a) the variations in the average number of total peaks per unit time, b) the total number of peaks and of zero level up-crossings per rotor revolution and c) the ranges of lower level thresholds within which $(\partial/\partial\xi)\, E[N_{+(\beta 1)}(\xi,t)]$ could be positive.

4) The areas under the curves of $p_{(\beta 1)}(\xi,t)$ for high level thresholds and of $E[M_{(T\beta 1)}(t)]$ are concentrated within two narrow azimuth-ranges per period which are centered at about the locations of the local maxima of $|y_{(\beta 1)}(0,t)|$. This observation further substantiates an earlier finding[1] that the response belongs to a quasi-coherent narrow-band process with small phase angle variance. High level peaks which cause significant damage to a structure[15,20] are most likely to occur within such narrow azimuth-ranges. Within and only within these two narrow azimuth-ranges, the Rayleigh density law is a satisfactory approximation to $p_{(\beta 1)}(\xi,t)$.

The preceding analysis remains valid for more comprehensive linear models of lifting rotor and input systems. However, under non-stationary random responses, the analyses and interpretation of reliability models on fatigue, ride roughness and response excursions are still in initial stages.[20] In spite of such gaps and other limitations due to linearization, the present study appears to be adequate to provide a quantitative description of the response process concerning peaks and narrow-band features. Particularly with the benefit of experimental results this study would also aid the development of realistic structural reliability models for unloaded rotors operating at high advance ratios.

References

[1]Gaonkar, G. H. and Hohenemser, K. H., "Stochastic Properties of Turbulence excited Rotor Blade Vibrations," *AIAA Journal*, Vol. 9, No. 3, March 1971, pp. 419–424.

[2]Gaonkar, G. H., Hohenemser, K. H. and Yin, S. K., "Random Gust Response Statistics for Coupled Torsion-Flapping Rotor Blade Vibrations," *Journal of Aircraft*, Vol. 9, No. 10, Oct. 1972, pp. 726–729.

[3]Barlow, J. B., "Theory of Propeller Forces in a Turbulent Atmosphere," Ph. D. thesis, May 1970, Institute for Aerospace Studies, University of Toronto.

[4]Jarosch, E. and Stepan, A., "Fatigue Properties and Test Procedures of Glass Reinforced Plastic Rotor Blades," *Journal of American Helicopter Society*, Vol. 15, No. 1, Jan. 1970, pp. 33–41.

[5]Cheney, M. C., "Results of Preliminary Studies of a Bearingless Helicopter Rotor Concept," *28th Annual National Forum of American Helicopter Society*, Paper 600, 1972.

[6]Gaonkar, G. H., "A General Method with Shaping Filters to Study Random Vibration Statistics of Lifting Rotors with Feedback Controls," *Journal of Sound and Vibration*, Vol. 21, No. 2, 1972, pp. 213–225.

[7]Sissingh, G. J., "Dynamics of Rotors Operating at High Advance Ratios," *Journal of American Helicopter Society*, Vol. 13, No. 3, 1968, pp. 56–63.

[8]Kuczynaski, W. A., Sharpe, D. L., and Sissingh, G. J., "Hingeless Rotor-Experimental Frequency Response and Dynamic Characteristics with Hub Moment Feedback Controls," *28th National Forum of American Helicopter Society*, Paper 612, 1972.

[9]Gaonkar, G. H. and Hohenemser, K. H., "Comparison of Two Stochastic Models for Threshold Crossing Studies of Rotor Blade Flapping Vibrations," AIAA Paper 71-389, Anaheim, Calif., 1971.

[10]Gaonkar, G. H. and Hohenemser, K. H., "An Advanced Stochastic Model for Threshold Crossing Studies of Rotor Blade Vibrations," *AIAA Journal*, Vol. 10, No. 8, Aug. 1972, pp. 1100–1101.

[11]Gault, J. D. and Gunter, D. E., "Atmospheric Turbulence Considerations for Future Aircraft Designed to Operate at Low Altitudes," *Journal of Aircraft*, Vol. 5, No. 6, Nov.-Dec. 1968, pp. 574–577.

[12]Gaonkar, G. H., "Interpolation of Aerodynamic Damping of Lifting Rotors in Forward Flight from Measured Response Variance," *Journal of Sound and Vibration*, Vol. 12, No. 3, 1971, pp. 381–389.

[13]Hohenemser, K. H. and Yin, S. K., "Some Applications of the Method of Multiblade Coordinates," *Journal of American Helicopter Society*, Vol. 17, No. 3, July 1972, pp. 3–12.

[14]Mil, M. L. et. al. "Helicopters-Calculation and Design," Vol. 1, *Aerodynamics*, TT F-519, May 1968, NASA.

[15]Lin, Y. K., *Probabilistic Theory of Structural Dynamics*, Chap. 9, McGraw-Hill, New York, 1967, pp. 292–330.

[16]Roberts, J. B., "Structural Fatigue Under Non-Stationary Random Loading," *Journal of Mechanical Engineering Science*, Vol. 8, No. 4, 1966, pp. 392–405.

[17]Howell, L. J. and Lin, Y. K., "Response of Flight Vehicles to Nonstationary Atmospheric Turbulence," *AIAA Journal*, Vol. 9, No. 11, Nov. 1971, pp. 2201–2207.

[18]Crandall, Stephen H., "Distribution of Maxima in the Response of an Oscillator to Random Excitation," *Journal of the Acoustical Society of America*, Vol. 47, No. 3(Pt. 2), 1971, pp. 838–845.

[19]Lin, Y. K., private communication, Nov. 1972, University of Illinois, Urbana, Ill.

[20]Freudenthal, A. M., ed., *International Conference on Structural Safety and Reliability*, 1st ed., Pergamon Press, New York, 1972, pp. 190–239.